nature chemistry

ARTICLES

PUBLISHED ONLINE: 3 APRIL 2011 | DOI: 10.1038/NCHEM.1012

# Biodegradable nanostructures with selective lysis of microbial membranes

Fredrik Nederberg[1†‡], Ying Zhang[2‡], Jeremy P. K. Tan[2‡], Kaijin Xu[3‡], Huaying Wang[3], Chuan Yang[2], Shujun Gao[2], Xin Dong Guo[4], Kazuki Fukushima[1], Lanjuan Li[3], James L. Hedrick[1*] and Yi-Yan Yang[2*]

**Macromolecular antimicrobial agents such as cationic polymers and peptides have recently been under an increased level of scrutiny because they can combat multi-drug-resistant microbes. Most of these polymers are non-biodegradable and are designed to mimic the facially amphiphilic structure of peptides so that they may form a secondary structure on interaction with negatively charged microbial membranes. The resulting secondary structure can insert into and disintegrate the cell membrane after recruiting additional polymer molecules. Here, we report the first biodegradable and *in vivo* applicable antimicrobial polymer nanoparticles synthesized by metal-free organocatalytic ring-opening polymerization of functional cyclic carbonate. We demonstrate that the nanoparticles disrupt microbial walls/membranes selectively and efficiently, thus inhibiting the growth of Gram-positive bacteria, methicillin-resistant *Staphylococcus aureus* (MRSA) and fungi, without inducing significant haemolysis over a wide range of concentrations. These biodegradable nanoparticles, which can be synthesized in large quantities and at low cost, are promising as antimicrobial drugs, and can be used to treat various infectious diseases such as MRSA-associated infections, which are often linked with high mortality.**

Bacteria are increasingly resistant to conventional antibiotics and, as a result, macromolecular peptide-based antimicrobial agents are now receiving a significant level of attention[1,2]. Most conventional antibiotics (such as ciprofloxacin, doxycycline and ceftazidime) do not physically damage the cell wall, but penetrate into the target microorganism and act on specific targets (for example, causing the breakage of double-stranded DNA due to inhibition of DNA gyrase, blockage of cell division and triggering of intrinsic autolysins). Bacterial morphology is preserved and, as a consequence, the bacteria can easily develop resistance. In contrast, many cationic peptides (for example, magainins, alamethicin, protegrins and defensins) do not have a specific target in the microbes, and instead interact with the microbial membranes through an electrostatic interaction, causing damage to the membranes by forming pores in them[3]. It is the physical nature of this action that prevents the microbes from developing resistance to the peptides. Indeed, it has been proven that cationic antimicrobial peptides can overcome bacterial resistance[4–6].

Most antimicrobial peptides have cationic and amphiphilic features, and their antimicrobial activities largely depend on the formation of facially amphiphilic α-helical[7–9] or β-sheet-like tubular[10] structures when interacting with negatively charged cell walls, followed by diffusion through the cell walls and insertion into the lipophilic domain of the cell membrane after recruiting additional peptide monomers. The disintegration of the cell membrane eventually leads to cell death. Over the last two decades, efforts have been made to design peptides with a variety of structures, but there has been limited success in clinical settings, and only a few cationic synthetic peptides have entered phase III clinical trials[1,11]. This is largely due to the cytotoxicity (for example, haemolysis) resulting from their cationic nature, their short half-lives *in vivo* (they are labile to proteases) and their high manufacturing costs[1].

A number of cationic polymers that mimic the facially amphiphilic structure and antimicrobial functionalities of peptides have been proposed as a better approach, because they can be prepared more easily and their synthesis can be more readily scaled up compared with peptides. For example, antimicrobial polynorbornene[12–14] and polyacrylate[15–17] derivatives, poly(arylamide)[18], poly($\beta$-lactam)[19] and pyridinium copolymers[20] have been synthesized either from amphiphilic monomers (homopolymers) or from a cationic (hydrophilic) monomer and hydrophobic comonomer (random copolymers). It was found that polymers prepared from amphiphilic monomers demonstrated a higher selectivity towards bacteria than towards red blood cells (mammalian cells)[20]. In addition, the overall hydrophobic/hydrophilic balance affected the antimicrobial activity and selectivity of the polymers[12,14,16]. However, most antimicrobial polymers reported in the literature are non-biodegradable, which limits their *in vivo* applications.

In this Article, we report the first biodegradable antimicrobial polymers. Unlike the existing antimicrobial polymers, which do not form a secondary structure before interacting with the microbial membrane, our polymers can readily form cationic micellar nanoparticles by direct dissolution in aqueous solution. The formation of nanostructures before coming into contact with the cell surface is expected to enable more efficient interaction with the cell membrane than is the case for individual polymer molecules. This is a result of the increased local mass and cationic charges of the nanostructures, which are important factors in the disintegration of the cell membrane through electroporation and/or the sinking raft model[21]. In addition, the large size of the micelles allows them to readily disintegrate the cell wall. Our previous studies have proved that an increased local concentration of cationic charge and peptide mass after the formation of nanostructures led to stronger antimicrobial activities[22].

[1]IBM Almaden Research Center, 650 Harry Road, San Jose, California 95120, USA, [2]Institute of Bioengineering and Nanotechnology, 31 Biopolis Way, Singapore 138669, Singapore, [3]State Key Laboratory for Diagnosis and Treatment of Infectious Diseases, First Affiliated Hospital, College of Medicine, Zhejiang University, 79 Qingchun Road, Hangzhou 310003, China, [4]School of Chemistry and Chemical Engineering, South China University of Technology, Guangzhou 510640, P. R. China; [†]Present address: DuPont Central Research and Development, Experimental Station, Wilmington, Delaware 19880, USA; [‡]These authors contributed equally to this work. *e-mail: hedrick@almaden.ibm.com; yyyang@ibn.a-star.edu.sg

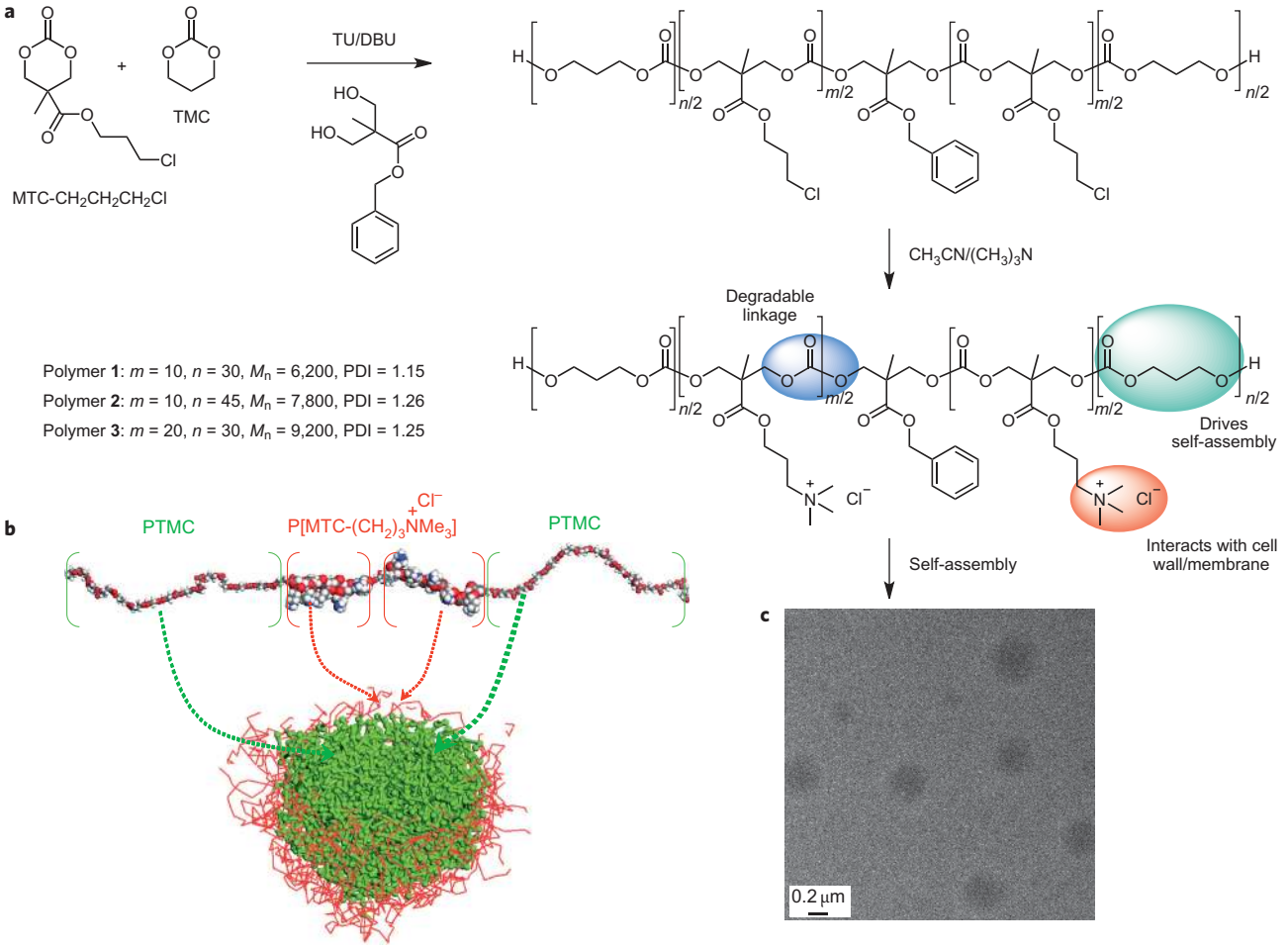


**Figure 1 | Synthesis and micelle formation of cationic amphiphilic polycarbonates. a**, Cationic amphiphilic polycarbonates were synthesized with a well-defined structure and narrow molecular weight distribution. Based on light scattering, zeta potential, TEM and simulation analyses, these polymers easily formed cationic micelles by direct dissolution in water. **b**,**c**, The formation of micelles was simulated through molecular modelling using Materials Studio Software (**b**) (in the polymer molecule: red, O; white, H; grey, C; blue, N), and was observed in a TEM image of polymer **3** (**c**) (scale bar, 0.2 μm).

Polycarbonates are attractive biomaterials because of their biocompatibility, biodegradability, low inherent toxicity and tunable mechanical properties[23–26]. We have recently developed a versatile living ring-opening polymerization (ROP) platform based on metal-free organocatalysis, which opens up a new route for synthesizing a variety of functional biodegradable polymers with predictable molecular weights and end-group fidelity[27,28]. In this study, we describe the synthesis and polymerization of functional cyclic carbonate to offer cationic amphiphilic triblock polycarbonates that exist in the form of cationic micellar nanoparticles in water. We demonstrate that these self-assembled nanoparticles are excellent antimicrobial drugs that selectively kill various microbes over mammalian red blood cells.

## Results and discussion

Cationic triblock polycarbonates with three different compositions were designed and synthesized (Fig. 1a) by the sequential ROP of the MTC–$(CH_2)_3$Cl monomer (3-chloropropyl 5-methyl-2-oxo-1,3-dioxane-5-carboxylate) followed by trimethylene carbonate (TMC) initiated from a diol in the presence of a mixture of the Lewis acid 1-(3,5-bis(trifluoromethyl)-phenyl)-3-cyclohexyl-2-thiourea (TU) and the Lewis base 1,8-diazabicyclo[5.4.0]undec-7-ene (DBU) as the catalyst. Quaternation of the central block with trimethylamine generated a cationic triblock copolymer containing two blocks of poly-TMC (PTMC) and one block of cationic poly-MTC (PMTC). The cationic PMTC block has a similar backbone structure to PTMC. The PTMC block was designed to drive self-assembly, and the cationic block was incorporated to interact with the microbial wall/membrane. These polycarbonates have narrow molecular weight distributions (listed in Supplementary Table S1), a feature that is crucial in future clinical applications, as individual molecular weight fractions of a polydisperse system are expected to exhibit distinct pharmacological activities *in vivo*[29]. Polymer **2** has a TMC (hydrophobic) block with a longer length than that in polymer **1**, whereas polymer **3** contains a longer length of cationic (hydrophilic) block than in polymer **1**.

No significant hydrolytic degradation was observed over 2 weeks for either polymer **1** or polymer **3** in water (Supplementary Fig. S1). It has been well established that aliphatic polycarbonates degrade via an enzymatic process, and *in vivo* degradation behaviour is different from that *in vitro*. For example, over 30 weeks, the weight of PTMC film decreased by only 9% *in vitro*[24]. However, in rats, although the degradation of PTMC film was still slow, it was more rapid than *in vitro*, as the degradation process was accelerated by an enzymatic process. The weight loss of PTMC in rats was 21.1% over 24 weeks. The degradation of polycarbonate produces an alcohol and carbon dioxide. Because of its slow degradation, PTMC has therefore been shown to have good biocompatibility *in vivo*[26]. In the case of antimicrobial polycarbonates, slow degradation may lead to prolonged antimicrobial functions. Furthermore, the slow *in vitro* hydrolytic degradation of polycarbonates means they have high stability and long shelf-lives.

Such polycarbonates easily form cationic micelles by simply dissolving in water, and polymers **1**, **2** and **3** have critical micelle concentrations (CMCs) of 35.5, 15.8 and 70.8 μg ml$^{-1}$ in deionized water, respectively (see Supplementary Figs S2–S4). In the buffer used for growing the bacteria in this study, the polymers have significantly lower CMC values (17.8, 11.2 and 28.2 μg ml$^{-1}$, respectively) due to the presence of salts in the buffer (Supplementary Figs S2–S4). Compared to polymer **1**, polymer **2**, with a relatively longer length of hydrophobic block, has a lower CMC due to the stronger hydrophobic interaction between polymer **2** molecules leading to micelle formation at lower concentrations. Polymer **3**, with its relatively longer length of hydrophilic block, has a higher CMC than polymer **1** because of the increased repulsive forces experienced by the longer hydrophilic block, which require more polymer molecules to come together to form a stronger hydrophobic interaction for micelle formation[30]. The average diameters of the micelles self-assembled from polymers **1** and **3** are 43 and 198 nm, respectively (Supplementary Table S1). Polymer **2**, with the hydrophobic block with the greatest length, forms large aggregates that have an average diameter of 402 nm. The micelles self-assembled from polymers **1**, **2** and **3** have positively charged surfaces with zeta potentials of 47, 65 and 60 mV, respectively.

The micelle formation of polycarbonate in aqueous solution was further demonstrated by means of coarse-grained simulation. This simulation offers a microscopic understanding of the thermodynamic properties and a detailed molecular model of the self-assembled micelles[31–33]. As illustrated by the simulation results (Fig. 1b), the hydrophobic block (green) assembles into the core of the spherical micelle, whereas the cationic block forms the shell (red). Transmission electron microscopy (TEM) images of polycarbonates in deionized water further prove that the micelles are spherical (Fig. 1c). These positively charged micelles can interact easily with the negatively charged surfaces of microbes by means of an electrostatic interaction, and can be taken up readily by the microbes.

Next, we evaluated the minimal inhibitory concentrations (MICs) of the polymers against Gram-positive bacteria such as *Bacillus subtilis*, *Enterococcus faecalis*, *Staphylococcus aureus* and methicillin-resistant *S. aureus* (MRSA), and the fungus *Cryptococcus neoformans*. MIC is an important parameter commonly used to evaluate the activity of new antimicrobial agents, and is generally defined as the minimum concentration of an antimicrobial agent at which no visible growth of microbes is observed[12–14,16,18–20]. Polymer **2** does not show an efficient inhibition effect on microbial growth, with an MIC of more than 64.0 μM against *B. subtilis* (Supplementary Fig. S5). This is because this polymer (with a hydrophobic block with the greatest length) precipitates when in contact with the growth medium.

In sharp contrast, polymers **1** and **3** have a strong effect against growth of the Gram-positive and drug-resistant Gram-positive bacteria, as well as the fungus. Their MIC values were cell-type-dependent. Polymer **1** has MIC values of 9.7, 6.5, 5.1, 16.0 and 16.0 μM against *B. subtilis*, *S. aureus*, MRSA, *E. faecalis* and *C. neoformans*, respectively (Supplementary Fig. S6). The equivalent MICs of polymer **3** are 4.3, 6.5, 7.0, 10.8 and 10.8 μM, respectively (Fig. 2), which are significantly lower than those of polymer **1**, especially for *B. subtilis*, *E. faecalis* and *C. neoformans*, probably because of the longer cationic blocks in each polymer **3** molecule. Interestingly, the MICs of polymers **1** and **3** against all types of microbes tested are higher than their CMCs in the buffer (that is, 17.8 μg ml$^{-1}$ = 2.9 μM and 28.2 μg ml$^{-1}$ = 3.1 μM, respectively). Individual polymer molecules are not potent enough to inhibit microbial growth. However, the formation of micelles increases the local concentration of cationic charge and polymer mass, leading to strong interactions between the polymer and cell wall/membrane, which may translate to effective antimicrobial activities.

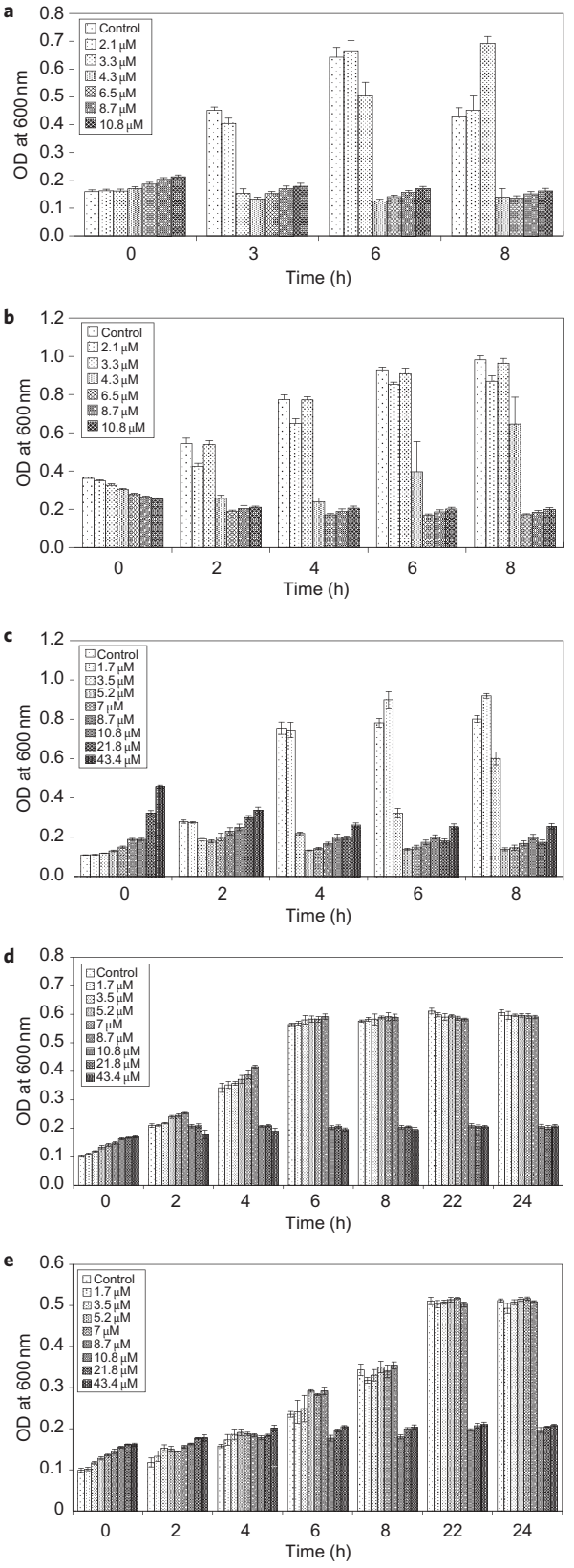


**Figure 2 | Dose-dependent growth inhibition of a range of bacteria and a fungus in the presence of polymer 3. a**, *Bacillus subtilis*. **b**, *Staphylococcus aureus*. **c**, MRSA. **d**, *Enterococcus faecalis*. **e**, *Cryptococcus neoformans*. Polymer **3** efficiently inhibited growth of these microbes with MICs of 4.3, 6.5, 7.0, 10.8 and 10.8 μM for **a**–**e**, respectively. The data are expressed as mean ± standard deviation of at least three replicates. Standard deviation is shown by the error bars. OD, optical density.

As a comparison, we tested the MICs of conventional antimicrobial agents that are used in clinical settings to treat infections caused by these microbes, such as vancomycin for *S. aureus*, MRSA and *E. faecalis*, and amphotericin B for *C. neoformans* (Supplementary Fig. S7). When compared with these conventional antimicrobial agents, the polymers demonstrated comparable antimicrobial activities against all the microbes except for *E. faecalis*. This is important, because vancomycin-resistant *E. faecalis*[34] and *S. aureus*[35,36], as well as amphotericin B-resistant *C. neoformans*[37] have been reported, and the resistant strains of these microbes are not susceptible to conventional antimicrobial agents. This suggests that there is an urgent need to develop safe and efficient macromolecular antimicrobial agents.

To study if the polymers are microbicidal at the concentration range corresponding to MICs and if the decreased MIC values observed in Fig. 2b,c as well as in Supplementary Fig. S6B,C were caused by the flocculation and precipitation of negatively charged microbes out of solution, we also conducted colony assays in the microbial samples treated with polymers **1** and **3** for 8 or 24 h, at various concentrations. As was the case when the microbes were treated with vancomycin and amphotericin B, both polymers killed ~100% of microbes at the concentration ranges corresponding to their MICs as well as at high concentrations (Supplementary Figs S8–S11). The reduced optical density values are not a result of flocculation or precipitation of live bacteria, but could be caused by aggregation of cationic micelles at high concentrations. Both polymers are therefore microbicidal.

To explore the mechanism of the antimicrobial action of the micelles, as an example we investigated the morphological changes in MRSA, *E. faecalis* and *C. neoformans* before and after incubation with the micelles formed from polymer **1** for 8 h at lethal doses (10.8 μM for MRSA and 16.3 μM for *E. faecalis* and *C. neoformans*, values slightly above the MICs). This was undertaken using TEM observations. As shown in Fig. 3, the cell walls and membranes of the microorganisms were damaged, and cell lysis was observed after treatment with the micelles. In addition, a large empty space was observed in the cytosol, as well as a burst of the cytoplast, in the treated *C. neoformans* samples.

We hypothesize that the cationic micelles can interact easily with the negatively charged cell wall by means of an electrostatic interaction, and the steric hindrance imposed by the mass of micelles in the cell wall and the hydrogen-binding/electrostatic interaction between the cationic micelle and the cell wall may inhibit cell wall synthesis[38] and/or damage the cell wall, resulting in cell lysis. In addition, the micelles may easily permeate the cytoplasmic membrane of the organisms due to the relatively large volume of the micelles[9], destabilizing the membrane as a result of electroporation and/or the sinking raft model[21], leading to cell death. To further study the interactions between the microbes and the polycarbonate micelles, we plan to incorporate a metal element into the polycarbonate in the future, which would allow clear visualization of the polymer nanoparticles within the microbes at different time points by means of TEM.

Haemolysis is a major harmful side effect of many cationic antimicrobial peptides and polymers. The haemolysis of mouse red blood cells was evaluated after incubation with polymers **1** and **3** at various concentrations. Although the polymers disrupt microbial walls/membranes efficiently (Fig. 3), they do not damage red blood cell membranes. Therefore, little haemolysis was observed, even at a concentration of 500 μg ml$^{-1}$ (81 and 54 μM for polymers **1** and **3**, respectively) (Supplementary Fig. S12), a concentration well above their respective MICs. The surfaces of Gram-positive bacteria and fungi are much more negatively charged than those of red blood cells[39]. Therefore, the electrostatic interaction between the surfaces of the bacteria/fungi and the cationic micelles is much stronger than that between the surfaces of the red blood cells and the cationic micelles, leading to excellent antimicrobial activity, but insignificant haemolytic activity.

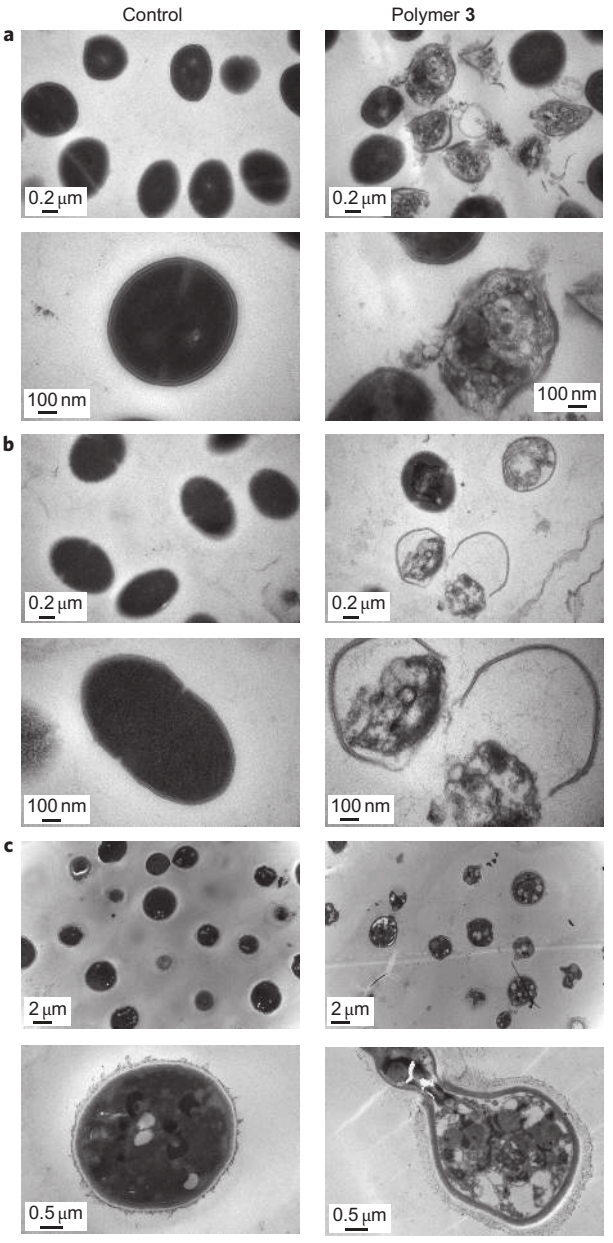


**Figure 3 | Comparative TEM images of microbes in the absence and presence of polymer 3. a–c**, MRSA (**a**), *Enterococcus faecalis* (**b**) and *Cryptococcus neoformans* (**c**) before (left) and after incubation (right) with polymer **3** for 8 h at lethal doses (10.8 μM for MRSA and 16.3 μM for *E. faecalis* and *C. neoformans*), values that are slightly above the MICs. After treatment, cell walls and membranes were damaged, and cell death was observed. In *C. neoformans*, large empty spaces were observed in the cytosol, as well as a burst of the cytoplast. In each lettered part of the figure, the bottom two images are magnified with respect to the top images. Scale bars: 0.2 μm (top) and 100 nm (bottom) (**a**,**b**); 2 μm (top) and 0.5 μm (bottom) (**c**).

To demonstrate the potential of the antimicrobial polymers in *in vivo* applications, we used polymer **1** as an example and evaluated its *in vivo* toxicity level. The $LD_{50}$ of polymer **1** (the lethal dose at which half the mice were killed) was determined to be 31.5 mg kg$^{-1}$ via intravenous injection. We also investigated the acute toxicity that the polymer might cause to major organs (the liver and kidney) and the balance of electrolytes in the blood by

**Table 1 | Effect of polymer 1 on liver and kidney functions as well as balance of electrolytes in the blood.**

| Treatment | ALT (U $l^{-1}$) | AST (U $l^{-1}$) | Creatinine (μmol $l^{-1}$) | Urea nitrogen (mmol $l^{-1}$) | Potassium ion (mmol $l^{-1}$) | Sodium ion (mmol $l^{-1}$) |
|---|---|---|---|---|---|---|
| Without treatment | 48.9±16.0 | 75.4±18.2 | 18.6±1.0 | 7.6±0.8 | 4.9±0.3 | 149.9±1.3 |
| | ($n$=10) | ($n$=10) | ($n$=10) | ($n$=10) | ($n$=10) | ($n$=10) |
| 48 h post-treatment | 42.6±4.0 | 67.9±12.2 | 20.1±3.3 | 8.0±1.1 | 5.0±0.9 | 148.9±1.9 |
| | ($n$=10) | ($n$=10) | ($n$=10) | ($n$=10) | ($n$=10) | ($n$=10) |
| | $P$=0.1 (>0.05) | $P$=0.2 (>0.05) | $P$=0.1 (>0.05) | $P$=0.2 (>0.05) | $P$=0.4 (>0.05) | $P$=0.1 (>0.05) |
| 14 days post-treatment | 40.6±9.5 | 75±20.5 | 19.3±4.5 | 7.4±1.3 | 4.8±0.3 | 150.0±0.9 |
| | ($n$=10) | ($n$=10) | ($n$=10) | ($n$=10) | ($n$=10) | ($n$=10) |
| | $P$=0.1 (>0.05) | $P$=0.5 (>0.05) | $P$=0.3 (>0.05) | $P$=0.4 (>0.05) | $P$=0.2 (>0.05) | $P$=0.1 (>0.05) |

The polymer causes no significant acute damage to the liver and kidney functions, nor does it interfere with the concentrations of potassium and sodium ions in the blood at a concentration well above the MICs of the polymer. The data are expressed as mean±standard deviation, based on values obtained from 10 mice ($n$=10). Statistical analysis was performed using Student's $t$-test. Differences are considered statistically significant with probability $P<0.05$. ALT, alanine transaminase; AST, aspartate transaminase; U, international unit.

analysing levels of alanine transaminase (ALT), aspartate transaminase (AST), creatinine, urea nitrogen, and sodium and potassium ions in blood samples obtained from treated mice 48 h post-injection. The levels of the functional parameters of the liver and kidney and the concentrations of potassium and sodium ions (Table 1) were unchanged 48 h after intravenous injection of polymer **1** at a concentration well above the MIC of the polymer (dose, 12 mg $kg^{-1}$; estimated concentration in the blood, 39 μM, assuming that the blood volume of the mouse is ~1 ml). This indicates that the micelles do not cause significant acute damage to liver and kidney functions, nor do they interfere with the electrolyte balance in the blood. Importantly, these parameters remain unchanged, even at 14 days post-injection. In addition, no mouse treated with the polymer died, and no colour change was observed in the serum samples and urine of the mice treated with the polymer when compared with the control group. These findings demonstrate that the polymer did not induce significant toxicity to the mice during the period of testing. Nonetheless, preclinical studies should be conducted in the future to further evaluate potential long-term toxicity of the antimicrobial polymers before clinical applications.

In conclusion, we have designed and synthesized novel biodegradable, cationic and amphiphilic polycarbonates that can easily self-assemble into cationic micellar nanoparticles by direct dissolution in water. The cationic nanoparticles formed from the polymers, with optimal compositions, can efficiently kill Gram-positive bacteria, MRSA and fungi, even at low concentrations. Importantly, they have no significant haemolytic activity over a wide range of concentrations, and cause no obvious acute toxicity to the major organs and the electrolyte balance in the blood of mice at a concentration well above the MICs. These antimicrobial polycarbonate nanoparticles could be promising as antimicrobial drugs for the decolonization of MRSA and for the treatment of various infectious diseases, including MRSA-associated infections.

## Methods

**Polymer synthesis.** The cationic amphiphilic polycarbonates were synthesized in three steps. First, MTC–COOH (8.82 g, 55 mmol) was converted to MTC–Cl using standard procedures with oxalyl chloride[24]. In a dry 250 ml round-bottomed flask equipped with a stir bar, the intermediate MTC–Cl was dissolved in 150 ml of dry methylene chloride. Under nitrogen flow, an addition funnel was attached in which chloro-propanol (4.94 g, 4.36 ml, 52.25 mmol), pyridine (3.95 g, 4.04 ml, 55 mmol) and 50 ml of dry methylene chloride was charged. The flask was cooled to 0 °C using an ice bath and the solution was added dropwise over 30 min. The ice bath was removed after a further 30 min and the formed solution stirred for an additional 16 h under nitrogen. The crude product was directly applied onto a silica gel column and the product purified by eluting with 100% methylene chloride. The product fractions were collected and the solvent evaporated, yielding the product as an off-white oil, which crystallized on standing. The yield was 11 g (85%). $^1$H NMR ($CDCl_3$) δ: 4.63 (d, 2H, $CH_2$), 4.32 (t, 2H, $CH_2$), 4.16 (d, 2H, $CH_2$), 3.55 (t, 2H, $CH_2$), 2.09 (m, 2H, $CH_2$), 1.25 (s, 3H, $CH_3$). HR-ESI-MS: $m/z$ calcd for $C_9H_{13}ClO_5$ + Na 259.0350; found 259.0353.

In the second step, MTC–$(CH_2)_3$Cl and TMC were copolymerized using a mixture of the Lewis acid TU and the Lewis base DBU (1:1 in mole) as the catalyst. In brief, in a glovebox, 93 mg (0.422 mmol) of benzyl protected bis-MPA diol initiator, 1.0 g (4.22 mmol) of MTC–$(CH_2)_3$Cl (for a degree of polymerization (DP) of 10) and 1.29 g (12.66 mmol) of TMC (for a DP of 30) was charged in a 20 ml glass vial equipped with a stir bar. Dichloromethane was added and the concentration was adjusted to 2 M. To initiate the polymerization, 80 mg (0.211 mmol) of TU and 32 mg (0.211 mmol) of DBU were added to the clear solution. After 5 h, 51 mg (0.422 mmol) of benzoic acid was added to quench the polymerization, after which the crude product was taken out off the glovebox and precipitated in cold methanol. The precipitate was allowed to sediment, and the supernatant was decanted. The collected polymer was dried in a vacuum oven until a constant weight was reached. Yield, ~2.1 g (~92%). Gel permeation chromatography: $M_w \approx 6{,}811$ g $mol^{-1}$, $M_n \approx 5{,}890$ g/$mol^{-1}$, polydispersity index (PDI) ≈ 1.15, $^1$H NMR ($CDCl_3$) δ: 7.41–7.35 (m, 5H, initiator), 5.19 (s, 2H, initiator), 4.40–4.30 (m, 6H, MTC-polymer), 4.30–4.18 (t, 4H, TMC-polymer), 3.76 (t, 4H, end-group), 3.61 (t, 2H, MTC-polymer), 2.18–2.12 (m, 2H, MTC-polymer), 2.12–2.00 (m, 4H, TMC-polymer), 1.92 (m, 4H, end-group), 1.28 (s, 3H, MTC-polymer).

Finally, the chloride functional polymer (2.0 g, ~0.4 mmol) was dissolved in acetonitrile (50 ml) and the solution transferred (under nitrogen) into a 100 ml pressure-safe Schlenk tube equipped with a stir bar. Under nitrogen, the solution was cooled with dry ice, after which trimethylamine (~0.5 g) was condensed into the Schlenk tube, which was then sealed. The solution was heated to 50 °C and held for 48 h while stirring. Following the reaction, the solution was cooled to ambient temperature, and nitrogen was bubbled through to remove excess trimethylamine. The solvent was removed by rotational evaporation, and the obtained product was dried in a vacuum oven until a constant weight was reached. $^1$H NMR (DMSO-d6) δ: 7.41–7.35 (m, 5H, initiator), 5.19 (s, 2H, initiator), 4.40–4.20 (m, 6H, MTC-polymer), 4.20–4.10 (t, 4H, TMC polymer), 3.50 (t, 4H, end-group), 3.50–3.40 (t, 2H, MTC-polymer), 3.10–3.0 (s, 9H, MTC-polymer), 2.10–2.0 (m, 2H, MTC-polymer), 2.0–1.90 (m, 4H, TMC-polymer), 1.85 (m, 4H, end-group), 1.22 (s, 3H, MTC-polymer). This reaction was quantitative.

Details on the protocols for CMC and MIC measurements, colony assays, TEM observations, haemolysis assays, *in vitro* polymer degradation and *in vivo* toxicity studies are described in the Supplementary Information.

Received 3 February 2010; accepted 17 February 2011; published online 3 April 2011

## References

1. Hancock, R. E. W. & Sahl, H. G. Antimicrobial and host–defence peptides as new anti-infective therapeutic strategies. *Nature Biotechnol.* **24,** 1551–1557 (2006).
2. Radzishevsky, I. S. *et al.* Improved antimicrobial peptides based on acyl-lysine oligomers. *Nature Biotechnol.* **25,** 657–659 (2007).
3. Brogden, K. A. Antimicrobial peptides: pore formers or metabolic inhibitors in bacteria. *Nature Rev. Microbiol.* **3,** 238–250 (2005).
4. Boman, H. G. Antibacterial peptides: key components needed in immunity. *Cell* **65,** 205–207 (1991).
5. Lehrer, R. I. & Ganz, T. Antimicrobial peptides in mammalian and insect host defense. *Curr. Opin. Immunol.* **11,** 23–27 (1999).
6. Hoffmann, J. A., Kafatos, F. C., Janeway, C. A. & Ezekowitz, R. A. Phylogenetic perspectives in innate immunity. *Science* **284,** 1313–1318 (1999).
7. Oren, Z. *et al.* Structures and mode of membrane interaction of a short α helical lytic peptide and its diastereomer determined by NMR, FTIR, and fluorescence spectroscopy. *Eur. J. Biochem.* **269,** 3869–3880 (2002).
8. Oren, Z. & Shai, Y. Cyclization of a cytolytic amphipathic α-helical peptide and its diastereomer: effect on structure, interaction with model membranes, and biological function. *Biochemistry* **39,** 6103–6114 (2000).

9. Shai, Y. Mode of action of membrane-active antimicrobial peptides. *Biopolymers (Peptide Science)* **66,** 236–248 (2002).
10. Fernandez-Lopez, S. *et al.* Antibacterial agents based on the cyclic D,L-α-peptide architecture. *Nature* **412,** 452–455 (2001).
11. Jerold Gordon, Y. & Romanowski, E. G. A review of antimicrobial peptides and their therapeutic potential as anti-infective drugs. *Curr. Eye Res.* **30,** 505–515 (2005).
12. Lienkamp, K. *et al.* Antimicrobial polymers prepared by ROMP with unprecedented selectivity: a molecular construction kit approach. *J. Am. Chem. Soc.* **130,** 9836–9843 (2008).
13. AL-Badri, Z. M. *et al.* Investigating the effect if increasing charge density on the hemolytic activity of synthetic antimicrobial polymers. *Biomacromolecules* **9,** 2805–2810 (2008).
14. Ilker, M. F., Nüsslein, K., Tew, G. N. & Coughlin, E. B. Tuning the hemolytic and antimicrobial activities of amphiphilic polynorbornene derivatives. *J. Am. Chem. Soc.* **126,** 15870–15875 (2004).
15. Kenawy, E.-R., Worley, S. D. & Broughton, R. The chemistry and application of antimicrobial polymers: a state-of-the-art review. *Biomacromolecules* **8,** 1359–1384 (2007).
16. Kuroda, K. & DeGrado, W. F. Amphiphilic polymethacrylate derivatives as antimicrobial agents. *J. Am. Chem. Soc.* **127,** 4128–4129 (2005).
17. Ivanov, I. *et al.* Characterization of nonbiological antimicrobial polymers in aqueous solution and at water–lipid interfaces from all-atom molecular dynamics. *J. Am. Chem. Soc.* **128,** 1778–1779 (2006).
18. Tew, G. N. *et al. De novo* design of biomimetic antimicrobial polymers. *Proc. Natl Acad. Sci. USA* **99,** 5110–5114 (2002).
19. Mowery, B. P. *et al.* Mimicry of antimicrobial host–defense peptides by random copolymers. *J. Am. Chem. Soc.* **129,** 15474–15476 (2007).
20. Sambhy, V., Peterson, B. R. & Sen, A. Antibacterial and hemolytic activities of pyridinium polymers as a function of the spatial relationship between the positive charge and the pendant alkyl tail. *Angew. Chem. Int. Ed.* **47,** 1250–1254 (2008).
21. Chan, D. I., Prenner, E. J. & Vogel, H. J. Tryptophan- and arginine-rich antimicrobial peptides: structures and mechanisms of action. *Biochim. Biophys. Acta Biomembranes* **1758,** 1184–1202 (2006).
22. Liu, L. H. *et al.* Self-assembled cationic peptide nanoparticles as an efficient antimicrobial agent. *Nature Nanotech.* **4,** 457–463 (2009).
23. Mei, H., Zhong, Z., Long, F. & Zhuo, R. Synthesis and characterization of novel glycol-derived polycarbonates with pendant hydroxyl groups. *Macromol. Rapid Commun.* **27,** 1894–1899 (2006).
24. Zhu, K. J., Hendren, R. W., Jensen, K. C. & Pitt, G. Synthesis, properties, and biodegradation of poly(1,3-trimethylene carbonate). *Macromolecules* **24,** 1736–1740 (1991).
25. Watanabe, J., Kotera, H. & Akashi, M. Reflective interfaces of poly(trimethylene carbonate)-based polymers: enzymatic degradation and selective adsorption. *Macromolecules* **40,** 8731–8736 (2007).
26. Edlund, U., Albertsson, A.-C., Singh, S. K., Fogelberg, I. & Lundgren, B. O. Sterilization, storage stability and *in vivo* biocompatibility of poly(trimethylene carbonate)/poly(adipic anhydride) blends. *Biomaterials* **21,** 945–955 (2000).
27. Nederberg, F. *et al.* Organocatalytic ring opening polymerization of trimethylene carbonate. *Biomacromolecules* **8,** 153–160 (2007).
28. Pratt, R. C., Nederberg, F., Waymouth, R. M. & Hedrick, J. L. Tagging alcohols with cyclic carbonate: a versatile equivalent of (meth)acrylate for ring-opening polymerization. *Chem. Commun.* 114–116 (2008).
29. Hunter, A. C. Molecular hurdles in polyfectin design and mechanistic background to polycation induced cytotoxicity. *Adv. Drug Deliv. Rev.* **58,** 1523–1531 (2006).
30. Deguchi, K. & Meguro, K. The determination of critical micelle concentrations of nonionic surfactants by charge-transfer solubilization of 7,7,8,8-tetracyanoquinodimethane. *J. Colloid Interface Sci.* **38,** 596–600 (1972).
31. Ryjkina, E., Kuhn, H., Rehage, H., Muller, F. & Peggau, J. Molecular dynamic computer simulations of phase behavior of non-ionic surfactants. *Angew. Chem. Int. Ed.* **41,** 983–986 (2002).
32. Guo, X. D., Zhang, L. J., Qian, Y. & Zhou, J. Effect of composition on the formation of poly(DL-lactide) microspheres for drug delivery systems: mesoscale simulations. *Chem. Eng. J.* **131,** 195–201 (2007).
33. Srinivas, G. & Pitera, J. W. Soft patchy nanoparticles from solution-phase self-assembly of binary diblock copolymers. *Nano Lett.* **8,** 611–618 (2008).
34. Barbara, E. & Murray, M. D. Vancomycin-resistant *Enterococcal* infections. *N. Engl. J. Med.* **342,** 710–721 (2000).
35. Chang, S. *et al.* Infection with vancomycin-resistant *Staphylococcus aureus* containing the *vanA* resistance gene. *N. Engl. J. Med.* **348,** 1342–1347 (2003).
36. Hiramatsu, K. Vancomycin-resistant *Staphylococcus aureus*: a new model of antibiotic resistance. *Lancet Infect. Dis.* **1,** 147–155 (2001).
37. Kelly, S. L. *et al.* Resistance to amphotericin B associated with defective sterol $\Delta^{8\rightarrow7}$ isomerase in a *Cryptococcus neoformans* strain from an AIDS patient. *FEMS Microbiol. Lett.* **122,** 39–42 (1994).
38. Cho, S. *et al.* Structural insights into the bactericidal mechanism of human peptidoglycan recognition proteins. *Proc. Natl Acad. Sci. USA* **104,** 8761–8766 (2007).
39. Som, A. & Tew, G. N. Influence of lipid composition on membrane activity of antimicrobial phenylene ethynylene oligomers. *J. Phys. Chem. B* **112,** 3495–3502 (2008).


## Acknowledgements

This research was supported by the National Science Foundation (NSF) Center for Polymer Interface and Macromolecular Assemblies (CPIMA; NSF-DMR-0213618) and the Institute of Bioengineering and Nanotechnology (Biomedical Research Council, Agency for Science, Technology and Research, Singapore). F.N. thanks the Swedish research council (VR) for financial support.

## Author contributions

J.L.H. and Y.Y.Y. conceived and designed the study. F.N., K.F. and C.Y. synthesized and characterized the polymers. Y.Z., J.P.K.T., K.X. and H.W. performed *in vitro* experiments, and S.G. carried out *in vivo* experiments. S.G., K.X., H.W. and L.L. contributed to *in vivo* data analysis. X.D.G. performed the simulation. J.L.H. and Y.Y.Y. wrote the paper, with contributions from the other authors for the Methods.

## Additional information

The authors declare no competing financial interests. Supplementary information accompanies this paper at www.nature.com/naturechemistry. Reprints and permission information is available online at http://npg.nature.com/reprintsandpermissions/. Correspondence and requests for materials should be addressed to J.L.H. and Y.Y.Y.